3D Face Recognition Based on Volumetric Representation of Range Image

Koushik Dutta, Debotosh Bhattacharjee, Mita Nasipuri and Anik Poddar

Abstract In this paper, a 3D face recognition system has been developed based on the volumetric representation of 3D range image. The main approach to build this system is to calculate volume on some distinct region of 3D range face data. The system has mainly three steps. In the very first step, seven significant facial landmarks are identified on the face. Secondly, six distinct triangular regions A to F are created on the face using any three individual landmarks where nose tip is common to all regions. Further 3D volumes of all the respective triangular regions have been calculated based on plane fitting on the input range images. Finally, KNN and SVM classifiers are considered for classification. Initially, the classification and recognition are carried out on the different volumetric region, and a further combination of all the regions is considered. The proposed approach is tested on three useful challenging databases, namely Frav3D, Bosphorous, and GavabDB.

Keywords Volumetric representation · 3D range image · Facial landmark Plane fitting · Classification

K. Dutta (✉) · D. Bhattacharjee · M. Nasipuri
Department of Computer Science and Engineering, Jadavpur University, Kolkata, West Bengal, India
e-mail: koushik.it.22@gmail.com

D. Bhattacharjee
e-mail: debotoshb@hotmail.com

M. Nasipuri
e-mail: mitanasipuri@gmail.com

A. Poddar
Computer Science Engineering, Birla Institute of Technology, Mesra, Ranchi, India
e-mail: apoddar2008@gmail.com

R. Chaki et al. (eds.), *Advanced Computing and Systems for Security*,
Advances in Intelligent Systems and Computing 883,
https://doi.org/10.1007/978-981-13-3702-4_11

1 Introduction

In the recent world, security is one of the most important issues in various fields due to a large amount of data hacking. Nowadays various social networking sites like Facebook and Twitter interact with us deeply. From the bad side of this interaction various risks like data leaks, Trojan, and impersonation may occur, where the personal information can be easily hacked by password hacking. On the other side, sometimes password and pin number are tough to properly memorize by us. To solve these types of issue, biometric-based verification and recognition system is used, which uses physical characteristic-based data. There are various biometrics like iris, fingerprints, face, and DNA. Among all of these verification or recognition system, face recognition system has taken significant attention from the researchers for the last few decades due to its various application domain like security, access control, and law enforcement. Face recognition [1] is possible in both 2D and 3D domain. 3D face recognition eliminates the problem like illumination and poses variation. As well as, working with 3D data gives extra geometrical information of face than a 2D face image. The methods are used for face recognition like holistic-based, feature-based, and hybrid-based approaches. The well-known holistic-based approaches are PCA [2, 3], LDA [4], and ICA [5]. The feature-based approaches include the extracted features from curvature analysis [6, 7] and structural matching-based features [8]. Finally some hybrid approaches [9, 10], which are basically the combination of holistic and feature-based approaches.

Feature extraction from images is very much challenging task in case of face recognition. It is difficult to extract innovative features from range images that recognize or verify person in the 3D domain. A large number of features can easily detect any person. Our main objective of this work is to represent the range image in a different form and also minimize the number of features that represent the face reliably. The alternative representation is essentially capturing the surface information.

The present system of 3D face recognition introduces a new approach for generating features by calculating the volume of the selected triangular regions on input range face images. All the significant contributions of this proposed work are enlisted below:

- Seven distinct landmarks are identified on significant portions like nose, eye, and mouth region of the input range face. Initially, the pronasal is chosen at the position, where curvedness and mean curvature both are maximum of multiple highest depth position. Next using the pronasal, other landmarks like eye and mouth corners are detected using the geometrical calculation of the face followed by mask representation for better localization.
- From those seven detected landmarks, three distinct landmarks are considered for the creation of one triangular region. In this way, six separate triangular regions are established.

- Next, the volume is calculated of all the triangular regions that produce a volumetric representation of the 2.5D face image. The volume is calculated by fitting plane on 3D range face image or 2.5D image.
- Finally, recognition accuracy of individual regions followed by merging of all separated regions is calculated successfully.

Volumetric representation of 3D range image is a new approach for calculating recognition rate. There are various other similar works that transform the original input range image to another form of 3D voxel representation and also other different formation. The voxel representation is basically the transformation of the original 3D mesh into a discrete and regular representation of a fixed number of volume elements or voxels. In [11], authors are presented new 3D voxel-based representation for face recognition. Here they have extracted three kinds of voxel representations: (1) those consisting of a single cut of the cube; (2) those consisting of a combination of single cuts of the cube; (3) depth maps. Support vector machine and PCA with Euclidean distance are used for matching the testing result. Pose and expression variant input images are considered for this work. Next in [12], the authors present a descriptor named as speed up local descriptor (SULD) from significant points extracted from the range image. They use frontal as well as pose variation images for the inputs of the proposed model. Significant points have been extracted by using Hessian-based detector. The SULD descriptor against all the significant points is computed for features creation. Another work in [13], where the authors have proposed a system where three different regions: eye, nose, and mouth separately classify the image. Initially, the whole range face image transforms to its local binary pattern (LBP) form. Further histogram of oriented gradient (HOG) is used for feature extraction. Here neutral, occlusion, and expression invariant images are considered as input.

The paper is organized as follows: Sect. 2 illustrates different steps of the proposed system. Next, Sect. 3 presents the result of our proposed work. After that Sect. 4 illustrates the comparative analysis with previous techniques. Conclusion and future work are given in Sect. 5.

2 The Present Proposed System

The present system is divided into five different stages. The stages are listed below:

- 3D Range Image Acquisition
- Smoothing
- Landmark Identification
- Volumetric Representation
- Classification

2.1 3D Range Image Acquisition

The range image is also named as a 2.5D image [14] or depth image. It contains depth value in the normalized range in between 0 and 255. In the range image, Z or depth value is mapped in the X-Y plane. Considering depth value as intensity, it looks like the gray level image. The range image is constructed from the 3D point cloud, which is captured by the 3D scanner. During this investigation, authors are considered range images of Frav3D, Bosphorous, and Gavab databases.

2.2 Smoothing

After capturing 3D point clouds, it consists of various noises like spike and holes. For removing spike from the range image, various different 2D filters can be used like: Gaussian smoothing filter, mean filter, median filter, and weighted median filter. Here the weighted median filter [15] is used for removing spike. The weighted median filter is same as a generalized median filter, where the mask of filter consists of a nonnegative integer weighted value.

2.3 Landmark Detection

In our work, landmark identification is a very crucial step for the creation of triangular region over the face. A landmark is a point which has a biological meaning that can identify faces differently. Generally, two types of a landmark can be detected. Hard-tissue landmarks lie on the skeletal and soft-tissue landmarks are on the skin and can be identified on the 3D point clouds or on range images. In human face total, 59 landmarks could be collected, but 20 of them are most famous.

Here, all total seven significant landmarks are considered such as pronasal (nose tip), left and right endocanthions (inner eye corner), left and right exocanthions (outer eye corner), and left and right chelions (mouth corner). All the detected landmarks cover important regions of the face. Various techniques are already implemented for landmark detection [16]. Here, for localization of the landmarks, different shape descriptors like coefficients of fundamental forms, mean and Gaussian curvature, maximum and minimum curvature, shape index and curvedness index are used. Here, for the nose tip detection, maximum depth measurement followed by curvedness index, mean curvature is used. The mean (K) and Gaussian curvature (H) is calculated from the first and second order derivative of input depth matrix as shown in Eq. 1. Further, curvedness index (CI) is calculated from the maximum (k_1) and minimum (k_2) curvatures shown in Eq. 2. P is a differentiable function $z = P(x, y)$, P_x is the first derivative of P with respect to x, and P_y is the first derivative of P with respect

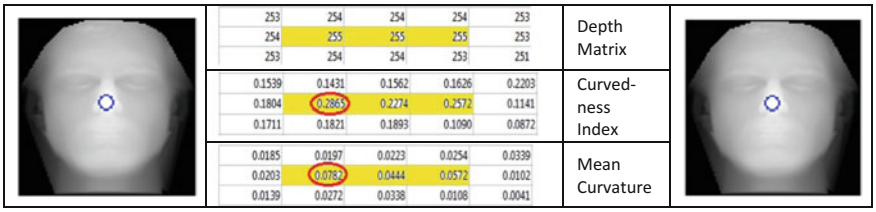

Fig. 1 Nose tip localization

to y. P_{xx} is the second derivative of P with respect to x, P_{yy} is the second derivative of P with respect to y and, finally, P_{xy} is the mixed derivative.

$$K = \frac{P_{xx}P_{yy} - P_{xy}^2}{\left(1 + P_x^2 + P_y^2\right)^2};\ H = \frac{\left(1 + P_x^2\right)P_{yy} - 2P_x P_y P_{xy} + \left(1 + P_y^2\right)P_{xx}}{\left(1 + P_x^2 + P_y^2\right)^{3/2}} \quad (1)$$

$$CI = \sqrt{\frac{k_1^2 + k_2^2}{2}} \quad \text{where} \quad k_1 = H + \sqrt{H^2 - K}; k_2 = H - \sqrt{H^2 - K} \quad (2)$$

Next, the geometric structure of the human face is considered for eye and mouth corner detection according to [17]. After the nose tip identification, rest of the landmarks are identified on the basis of nose tip. There is a geometrical relationship between nose tip and eye corners as well as mouth corners. Here, a circle is considered of radius say R around the nose tip point (a, b) as a center. The geometrical formulae for the detection of all other landmarks against the nose tip are shown in Eq. 3. Here, Ø is the angle between nose tip and other landmark point and (x, y) is the point of the proposed landmark.

$$x = R\cos\theta + a; \quad y = R\sin\theta + b \quad \text{where} \quad \theta = (pi/180) * Ø \quad (3)$$

After finding the points, in some of the cases the detected points are not accurate. So, the authors are concentrated for accurate localization for the landmarks. A mask of 7 × 7 is considered around the point and then examined all types of surface descriptor and derivative values on that mask. It is finding a way for appropriate localization of mouth and eye corners. The details of the landmark detection are given below.

Pronasal: Nose tip or pronasal is one of the most important facial landmark points, where depth value is maximum. In some cases, maximum depth value occurs multiple times in connected pixels of depth matrix. In that case, a new approach has taken to calculate curvedness index and mean curvature on those pixels and consider the point where both curvedness index and mean curvature are maximum. In Fig. 1, red mark identifies the point, where curvedness index and mean curvature are maximum.

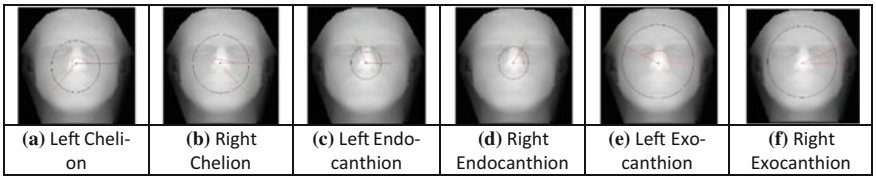

Fig. 2 Mouth, inner and outer eye corner localization

Chelion: Mouth corners or chelion are the landmark locations on the mouth. According to [17], consider a circle of radius r ($15 \leq r \leq 25$) pixels drawn around the center on nose tip. Further, left mouth corner located at the angle $\theta_1(220 \leq \theta_1 \leq 240)$ left of the nose tip on the circumference and right mouth corner located at the angle $\theta_2(300 \leq \theta_2 \leq 320)$ on the circumference. Figure 2a, b shows the left and right mouth corner landmark.

After getting the left and right mouth corner points, optimize the point consider 7×7 mask around the point.

Step 1: Consider the points, whose shape index belongs to range of Saddle surface, i.e., $[-0.125, 0.125)$
Step 2: Take the points where the first order derivative of z with respect to x greater than zero for left mouth corner and less than zero for right mouth corner
Step 3: The minimum of g of first fundamental form gives the left and right mouth corners

Endocanthion: Inner eye corners or endocanthions are the points where upper and lower inner eyelid meets. According to [17], a circle of radius r ($10 \leq r \leq 15$) draws around the center on nose tip. Further, left mouth corner located the angle $\theta_1(110 \leq \theta_1 \leq 130)$ left of the nose tip on the circumference and right mouth corner located at the angle $\theta_2(50 \leq \theta_2 \leq 70)$ on the circumference. Figure 2c, d shows the left and right inner eye corner landmark.

Similarly, after getting the left and right inner eye corner points, the following steps are considered for optimization of point using 7×7 mask around the point.

Step 1: Consider the points, whose shape index belongs to range of Ridge surface, i.e., [0.375, 0.625)
Step 2: Take the points where the first order derivative of z with respect to x greater than zero for both right and left eye
Step 3: The coefficients f and F of first and second fundamental forms greater than zero for the left eye and less than zero for the right eye
Step 4: The minimum of e of first fundamental form gives the left and right eye corner points

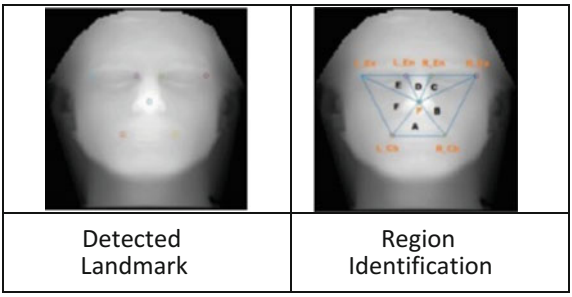

Fig. 3 Triangular regions against detected landmarks

Exocanthion: Outer eye corners or exocanthions are the points where upper and lower outer eyelid meets. According to [17], consider a circle of radius r ($25 \leq r \leq 35$) pixels drawn around the center on nose tip. Further, left outer eye corner is located at approximately $\theta_1 (150 \leq \theta_1 \leq 170)$ left of the nose tip on the circumference and right outer eye corner is located the angle $\theta_2 (10 \leq \theta_2 \leq 30)$ on the circumference. Figure 2e, f shows the left and right outer eye corner landmark.

Similar as before, after getting the left and right outer eye corner points, the following steps are considered for optimization of point using 7×7 mask around the point.

Step 1: Consider the points, whose shape index belongs to the range of Rut surface, i.e., $[-0.625, -0.375)$
Step 2: Take the points where the first order derivative of z with respect to x greater than zero for both right and left eye
Step 3: Divide the points of the first order derivative of z with respect to y into two clusters using K-means clustering technique. Consider the cluster of lower center value
Step 4: The points where Gaussian curvature K equal to zero and mean curvature less than zero
Step 5: The minimum of e of first fundamental form gives the left and right eye corner points

2.4 Volumetric Representation

This section is divided into two subsections: Triangular region identification and volume calculation.

Triangular Region Identification. After the landmark detection stage, the triangular region has been created based on three individual landmarks. According to the seven significant landmarks, all total six triangular regions: A, B, C, D, E, and F have built. The triangular region can be identified as from Fig. 3:

- Region A: ∇PL_ChR_Ch
- Region B: ∇PR_ChR_Ex

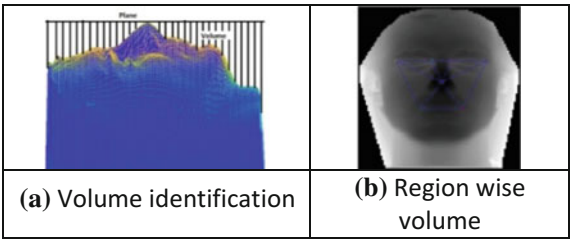

Fig. 4 Volume calculation on separate regions

- Region C: ∇PR_EnR_Ex
- Region D: ∇PL_EnR_En
- Region E: ∇PL_ExL_En
- Region F: ∇PL_ChL_Ex

Here 'P' denotes pronasal, L_Ch and R_Ch denote left and right chelion, L_En and R_En denote left and right endocanthions, and L_Ex and R_Ex denote left and right exocanthions. The DDA line drawing [18] algorithm is used for the creation of line between two distinct landmark points on range face image. All total six triangular regions cover a maximum portion of the face. Figure 3 illustrates all the triangular regions against different landmarks.

Volume Calculation. Volumetric representation gives the volume of the portion of the range face image. Volume is calculated on the triangular region A, B, C, D, E, and F separately. To measure the volume, at first a plane is fitted at the position of maximum depth (i.e., nose tip) of the range image. After plane fitting, the authors have calculated the distance between the plane and all other pixels of the face region as shown in Fig. 4a. The distance between maximum depth plane and other pixels is also treated as height or density of that pixel. Further, the summation of density is calculated the volume of any particular region. The resultant inverse range image is also named as density range image that gives the volume of the image. The volume of the entire separate region shown in Fig. 4b is calculated in the same way. Volume is calculated on all the six distinct regions, which is identified as features of any subject face.

Volume calculation of triangular region of density range image is done based on the scanline approach of computer graphics. Moreover, considering the triangular region, three information needed to be known for volume calculation of any region:

- Choosing of starting point
- Choose row-wise or column-wise scanline approach
- Farthest point detection in between other two points.

In our work, the authors are considered nose tip point or pronasal point of the face as the starting point because this point is common in all the triangular regions. Three cases according to the x and y position of the points occur before applying scanline approach as shown in Fig. 5. From the figure, according to the image axis if the x value of two other points (excluding starting point) is on the same side, it

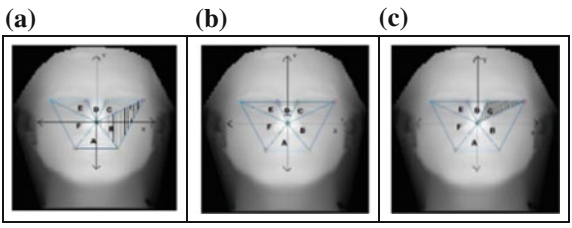

Fig. 5 Different cases of scanline technique

may be increasing or decreasing, and y value is on different sides than considering column-wise scanline approach as shown in Fig. 5a. Similarly, when the y value of two other points (excluding starting point) is on the same side, it may be increasing or decreasing, and x value is on different sides than considering row-wise scanline approach as in Fig. 5b. In some cases, when both x and y values are either increasing or decreasing than any approach can be considered as in Fig. 5c.

Another problem may also arise at the time of calculation that is the number of the index of the line array is not same as x value or y value difference. Due to the aliasing effect of a line drawing of the triangular region this problem has occurred. Now, the steps for volume calculation of any triangular region are given below.

Step 1: Take three points of the triangular region of the density range image
Step 2: Spatial coordinate vectors of line drawing between two points are taken
Step 3: Choose the starting point according to the problem. Here, pronasal is considered
Step 4: Check the position of the other two points. After that choose the scanline approach: row wise or column wise
Step 5: Add the density value according to one scanline. Then jump to next scanline and then one after another. In this way add the total density values. After this addition, the volume of any triangular region is calculated

The proposed work of volumetric representation can be mathematically justified by volume integral. It can be usually denoted as in Eq. 4.

$$\int_V f(x, y, z) d\tau \tag{4}$$

Here $f(x, y, z)$ denoted as z value of (x, y) location of the negative range image, which is basically identified as distance between highest depth plane and any particular pixel. Function is basically the summation of all pixels in a particular region. Let a, b, and c are the sides of the triangle and A denotes area of the circle. Equations 5 and 6 illustrate volume of the triangular region in this work.

$$A = \sqrt{S(S-a)(S-b)(S-c)} \quad \text{where } S = \frac{(a+b+c)}{2} \tag{5}$$

Table 1 Details of input databases

Database	Year	No. of subjects	No. of scans	Variation
Bosphorous [19]	2008	105 (60-M, 45-F)	4652	Pose, expression, occlusion
FRAV3D [20]	2006	106	1696	Pose, expression, illumination
GavabDB [21]	2004	61 (45-M, 16-F)	427	Smile, frontal accentuated laugh, frontal random gesture

$$V = \int_{Z_1}^{Z_2} A dz, \text{ where } Z_1 \text{ and } Z_2 \text{ are density value} \tag{6}$$

2.5 Classification

For classification, support vector machine (SVM) and K-nearest neighbour (KNN) classifiers were used. For the KNN, Euclidean distance is used for nearest distance calculation. Here twofold cross-validation technique is applied on input dataset, where the whole dataset is divided into two separate regions: training and test set.

3 Experiment and Result

The proposed work is tested on range images of three well-known databases Frav3D, Bosphorous, and GavabDB. The details of these databases are given below in Table 1.

The 3D data of these databases have been captured by the available 3D scanner. Initially 3D point cloud, further it is transformed to range images. Here in our work, only frontal faces including neutral and expression variation range images of size 100×100 are considered. At first, the accuracy of landmark localization compared to Bagchi et al. [17] is illustrated in Table 2. The standard deviation error (SDE) of seven distinct landmark localization of our proposed method and Bagchi et al. work comparable with the ground truth is represented. The 4 neutral and 2 expression variation images of FRAV3D, 2 neutral, 6 expression, 20 lower face AU (Action Units) (LFAU), 5 upper face AU (UFAU) and 2 Combined AU (CAU) of Bosphorous and 2 neutral and 2 expression face images of Gavab database are considered for landmark localization and further recognition. Here the recognition accuracy is calculated on separate regions. Further, the average of all distinct region's recognition accuracy correspond to the recognition accuracy of whole face region. Tables 3 and 4 given below illustrate the recognition rates of three databases using KNN and SVM classifier.

Table 2 Standard Deviation Error of proposed landmarks

Database	Variation	SDE (Proposed work)							SDE (Bagchi et al. [17])						
		P	L_Ch	R_Ch	L_En	R_En	L_Ex	R_Ex	P	L_Ch	R_Ch	L_En	R_En	L_Ex	R_Ex
FRAV3D	Neutral	0.33	4.24	2.5	3.14	3.78	2.27	3.98	0.35	3.98	2.13	4.36	3.53	3.43	5.66
	Expression	0.5	6.82	4.42	3.14	3.32	1.66	2.54	0.61	6.6	5	3.28	3.67	3.12	3.79
BOSPHORUS	Neutral	0.6	3.65	4.72	4.77	4.23	2.3	3.1	0.65	3.2	5.21	5.32	4.78	4.56	4.13
	Expression	0.55	5.41	6	3.28	2.89	4.3	2.98	0.4	5.74	6	4.87	4	5.47	4.23
	CAU	0.32	6.5	5.55	4.1	3.7	2.16	3.67	0.3	6.8	5.28	5.3	4.23	2.35	4.79
	LFAU	0.53	6.3	4.56	3.12	2.59	3.3	2.98	0.6	7.1	4.23	4.22	4	3.9	3.14
	UFAU	0.2	5.33	3.88	2.73	3	5.77	3.21	0.22	5	4.1	3.64	3.11	7.31	4.68
GAVAB	Neutral	0.3	3.86	2.56	2.87	3.7	1.5	2.34	0.32	4	2.44	3.11	3.72	3.2	3.35
	Expression	0.41	4.25	3	5.48	4.71	2.11	3.19	0.38	4.75	4.1	7.7	5.23	4.15	4.63

Table 3 Recognition accuracy of three input databases using KNN classifier

Database	Region A	Region B	Region C	Region D	Region E	Region F	Average
Frav3D	94.4	93.8	94	94.9	94.6	94	94.28
Bosphorous	95.88	95	94.77	95.45	95	95.2	95.21
GavabDB	91.68	90.3	91	90.6	91.4	90	90.83

Table 4 Recognition accuracy of three input databases using SVM classifier

Database	Region A	Region B	Region C	Region D	Region E	Region F	Average
Frav3D	95.58	95.3	96	95.9	95.78	95	95.59
Bosphorous	96.87	96	96.7	96	96.5	96.2	96.37
GavabDB	93.68	91.3	92	93.8	91.89	92.4	92.51

Table 5 Comparison of recognition performance of the proposed method with some other methods on the Frav3D database

Methods	Accuracy (%)	References
Curvature analysis + SVD + ANN (Classification on the whole face)	86.51	Ganguly et al. [6]
LBP + HOG + KNN (Region-based classification)	88.86	Dutta et al. [13]
Geodesic texture wrapping + Euclidean-based classification (Classification on the whole face)	90.3	Hajati and Gao [22]
ICP-based registration + Surface Normal + KPCA	92.25	Bagchi et al. [10]
Proposed Method (Triangular representation + Volume calculation + KNN)	**94.28**	This paper
DWT + DCT + PCA + Euclidean distance classifier	94.50	Naveen and Mon [23]
Proposed Method (Triangular representation + Volume calculation + SVM)	**95.59**	This paper

4 Comparative Study and Analysis

In our proposed work, Frav3D, Bosphorous, and Gavab databases are used as input database. There are already few works have already done on these databases. The comparison studies with previous other tasks of the three different databases: Frav3D, Bosphorous, and Gavab have been discussed in Tables 5, 6, and 7, respectively.

The recognition accuracies of our proposed method on Frav3D, Bosphorous, and Gavab database are 94.28%, 95.21%, and 90.83%, respectively, using KNN classifier and 95.59%, 96.37%, and 92.51%, respectively, using SVM classifier. Compare with other works, it can be established that our proposed work has not covered whole face region, whereas the existing proposed works of different authors had worked with whole face region. On the other side, the size of the feature set is short compared to other methods. On that basis it can say, the proposed system is more accurate.

Table 6 Comparison of recognition performance of the proposed method with some other methods on the Bosphorous database

Methods	Accuracy (%)	References
ICP-based recognition	89.2	Dibeklioglu et al. [24]
Proposed Method (Triangular representation + Volume calculation + KNN)	**95.21**	This paper
ICP-based holistic approach + Maximum likelihood classifier	95.87	Alyuz et al. [25]
Surface Normal and KPCA	96.25	Bagchi et al. [10]
Proposed Method (Triangular representation + Volume calculation + SVM)	**96.37**	This paper

Table 7 Comparison of recognition performance of the proposed method with some other methods on the Gavab database

Methods	Accuracy (%)	References
Mean and Gaussian curvature-based Segmentation	77.9	Moreno et al. [26]
Geometrical feature + PCA versus SVM classification	90.16	Moreno et al. [3]
Proposed Method (Triangular representation + Volume calculation + KNN)	**90.83**	This paper
2DPCA + SVM classifier	91	Mousavi et al. [27]
Proposed Method (Triangular representation + Volume calculation + SVM)	**92.51**	This paper

5 Conclusion

Here a new technique has been presented for 3D face recognition, where a new representation of range images has produced by calculating the volume of the regions of the face. Initially, landmarks are identified in an optimum way. The further triangular region has constructed by calculating line DDA algorithm. Next, a new algorithm has presented for calculating the volume of the selected triangular regions. The volumes of all distinct regions are used to construct feature vectors for classification. Overall it can be concluded that the volume representation of range images is a new approach in the 3D domain. The system is computationally efficient for recognition with high recognition accuracy. Frontal faces including neutral and expression variant range images of three well-known databases are used as input to this system. In the future, pose variant images will be considered for this technique.

Acknowledgements I, Koushik Dutta, would like to express thanks to Ministry of Electronics and Information Technology (MeitY), Govt. of India. I am also thankful for Department of Computer Science and Engineering, Jadavpur University, Kolkata, India for providing the necessary infrastructure for this work.

References

1. Abate, F., Nappi, M., Riccio, D., Sabatino, G.: 2D and 3D face recognition: a survey. Pattern Recogn. Lett. **28**(14), 1885–1906 (2007)
2. Gervei, O., Ayatollahi, A., Gervei, N.: 3D face recognition using modified PCA methods. World Acad. Sci. Eng. Technol. **4**(39), 264 (2010)
3. Moreno, A.B., Sanchez, A., Velez, J.F., Diaz, J.: Face recognition using 3D local geometrical features: PCA vs SVM. In: Proceedings of the ISPA, pp. 185–190 (2005)
4. Heseltine, T., Pears, N., Austin, J.: Three-dimensional face recognition: a fisher surface approach. In: Proceedings of the ICIAR, pp. 684–691 (2008)
5. Hesher, C., Srivastava, A., Erlebacher, G.: A novel technique for face recognition using range imaging. In: Proceedings of the Seventh International Symposium on Signal Processing and Its Applications, pp. 201–204 (2003)
6. Ganguly, S., Bhattacharjee, D., Nasipuri, M.: 3D face recognition from range images based on curvature analysis. ICTACT J. Image Video Process. **4**(03), 748–753 (2014)
7. Ganguly, S., Bhattacharjee, D., Nasipuri, M.: Fuzzy matching of edge and curvature based features from range images for 3D face recognition. Intell. Autom. Soft Comput. (IASC) **23**(1), 51–62 (2017)
8. Berretti, S., Werghi, N., Bimbo, A., Pala, P.: Matching 3D face scans using interest points and local histogram descriptors. Special section on 3D object retrieval. Comput. Graph. **37**, 509–525 (2013)
9. Chouchane, A., Belahcene, M., Ouamane, A., Bourannanae, S.: 3D face recognition based on histogram of local descriptors. In: 4th International Conference on Image Processing Theory, Tools and Applications (IPTA), pp. 1–5 (2014)
10. Bagchi, P., Bhattacharjee, D., Nasipuri, M.: 3D face recognition using surface normals. In: TENCON 2015—2015 IEEE Region 10 Conference, pp. 1–6 (2015)
11. Moreno, A.B., Sanchez, A., Velez, J.F.: Voxel-based 3D face representations for recognition. In: 12th International Workshop on Systems, Signals and Image Processing, pp. 285–289 (2005)
12. Shekar, B.H., Harivinod, N., Kumara, M.S., Holla, K.R.: 3D face recognition using significant point based SULD descriptor. In: International Conference on Recent Trends in Information Technology (ICRTIT) (2011)
13. Dutta, K., Bhattacharjee, D., Nasipuri, M.: Expression and occlusion invariant 3D face recognition based on region classifier. In: 1st International Conference on Information Technology, Information Systems and Electrical Engineering (ICITISEE), pp. 99–104 (2016)
14. Ganguly, S., Bhattacharjee, D., Nasipuri, M.: 2.5D face images: acquisition, processing and application. In: ICC 2014—Computer Networks and Security, pp. 36–44 (2014)
15. Yin, L., Wang, R., Neuvo, Y.: Weighted median filters: a tutorial. IEEE Trans. Circuits Syst. 11: Analog Digit. Signal Process. **43**(3) (1996)
16. Ahdid, R., Taifi, K., Safi, S., Manaut, B.: A survey on Facial Features Points Detection Techniques and Approaches. Int. J. Comput. Electr. Autom. Control Inf. Eng. **10**(8), 1566–1573 (2016)
17. Bagchi, P., Bhattacharjee, D., Nasipuri, M.: A robust analysis, detection and recognition of facial features in 2.5D images. Multimed. Tools Appl. **75**, 11059–11096 (2016)
18. DDA Line Drawing. http://www.geeksforgeeks.org/dda-line-generation-algorithm-computer-graphics/
19. Bosphorous. http://bosphorus.ee.boun.edu.tr/default.aspx
20. FRAV3D. http://www.frav.es/databases
21. GavabDB. http://gavab.escet.urjc.es/recursos_en.html
22. Hajati, F., Gao, Y.: Pose-invariant 2.5D face recognition using geodesic texture warping. In: 11th International Conference on Control, Automation, Robotics and Vision Singapore, pp. 1837–1841 (2010)
23. Naveen, S., Moni, R. S.: A robust novel method for Face recognition from 2D depth images using DWT and DCT fusion. In: International Conference on Information and Communication Technologies (ICICT), pp. 1518–1528. Elsevier (2014)

24. Dibeklioglu, H., Gokberk B., Akarun, L.: Nasal region-based 3D face recognition under pose and expression variations. In: ICB'09: Proceedings of the Third International Conference on Advances in Biometrics, pp. 309–318. Springer, Berlin, Heidelberg (2009)
25. Alyuz, N., Gokberk, B., Akarun, L.: A 3D face recognition system for expression and occlusion invariance. In: BTAS'08: Proceedings of the IEEE Second International Conference on Biometrics Theory, Applications and Systems, Arlington, Virginia, USA (2008)
26. Moreno, A.B., Sanchez, A., Velez, J.F., Diaz, J.: Face recognition using 3D surface-extracted descriptors. In: Irish Machine Vision and Image Processing Conference (2003)
27. Mousavi, M.H., Faez, K., Asghari, A.: Three dimensional face recognition using SVM classifier. In: Seventh IEEE/ACIS International Conference on Computer and Information Science, Portland, pp. 208–213 (2008)